SYNTHESIS OF $(NH_4)_xWO_3$ NANORODS BY A NOVEL HYDROTHERMAL ROUTE

SINTEZA $(NH_4)_xWO_3$ NANOPALČK Z NOVIM HIDROTERMALNIM POSTOPKOM

Xianguo Luo[1], Shubin Zhu[1], Xuhong Su[1], Jianguo Huang[1], Zekun Zhou[1], Qiongyu Zhou[2], Yufeng Wen[3], Ping Ou[1*]

[1]Jiangxi University of Science and Technology, School of Materials Science and Engineering, Hongqi Ave. No. 86, Ganzhou Jiangxi 341000, China
[2]Foshan University, School of Materials Science and Energy Engineering, Jiangwan Road No. 18, Foshan Guangdong 528000, China
[3]Jinggangshan University, School of Mathematical Sciences and Physics, Xueyuan Road No. 28, Ji'an Jiangxi 343009, China

We report on a novel hydrothermal route for synthesizing ammonium tungsten bronze $((NH_4)_xWO_3)$ nanorods. As-prepared $(NH_4)_xWO_3$ nanorods have an average diameter of 150 nm and length of 2 μm. These single-crystalline nanorods are hexagonal and grow along the c-axis. The formation process of the $(NH_4)_xWO_3$ nanorods is also discussed based on time-dependent experimental results.

Keywords: hydrothermal, $(NH_4)_xWO_3$, nanorod

Avtorji v pričujočem članku poročajo o novem hidrotermalnem postopku za sintezo nanopalčk amonijevega volframata $((NH_4)_xWO_3)$. Pripravljene nanopalčke $(NH_4)_xWO_3$ so imele povprečni premer 150 nm in dolžino 2 μm. Te monokristalinične nanopalčke imajo heksagonalno strukturo in rastejo vzdolž c-osi. Potek procesa tvorbe $(NH_4)_xWO_3$ nanopalčk avtorji opisujejo na osnovi časovno odvisnih preizkusov.

Ključne besede: hidrotermalni postopek, $(NH_4)_xWO_3$, nanopalčke

1 INTRODUCTION

Hexagonal tungsten bronzes are a group of non-stoichiometric compounds with the general formula M_xWO_3 (M=Cs, K, Na, Rb, NH4, etc.) that consists of mixed-valence tungsten ions (W^{6+} and W^{5+}). M_xWO_3 particles have been demonstrated to exhibit excellent near-infrared (NIR) absorption properties when dispersed in a one-dimensional form due to their unique surface electronic structures and crystallographic defects.[1–6] The designed growth of $(NH_4)_xWO_3$ nanorods is of great significance because they also exhibit mixed-valence tungsten ions and show NIR shielding abilities. Additionally, a substitution of alkali metal tungsten bronzes with $(NH_4)_xWO_3$ can avoid the consumption of alkali metals, especially the expensive Cs. Furthermore, owing to the open-tunnel structure and special electronic properties of $(NH_4)_xWO_3$, the mobility of the cations in the channels of the WO_3 framework allows a dramatic modification of their electronic properties due to ion exchange or intercalation, giving the $(NH_4)_xWO_3$ species broad application prospects as catalytic, battery, gas sensing and electrochromic materials.[7]

Unfortunately, due to the high structural distortion of $(NH_4)_xWO_3$ as a result of the insertion of large NH^{4+} ions into the WO_6 octahedral framework, it is still fairly difficult to synthesize. Until now, there have been few reports on the synthesis of one-dimensional $(NH_4)_xWO_3$. S. Guo et al.[6] reported a solvothemal method for preparing $(NH_4)_xWO_3$ nanorods at 200 °C for 72 h. However, the practical applications of this process are limited by complicated procedures, long reaction times and the use of expensive and environmentally unfriendly organic solvents. Consequently, exploiting simple, mild, low-cost routes for the preparation of $(NH_4)_xWO_3$ is quite imperative and exceedingly challenging.

In this work, we propose a novel, simple hydrothermal route for synthesizing $(NH_4)_xWO_3$ nanorods at 200 °C for 12 h, with sodium tungstate dihydrate ($Na_2WO_4 \cdot 2H_2O$), thiourea (CH_4N_2S) and citric acid monohydrate ($C_6H_8O_7 \cdot H_2O$) as the starting materials. Single-crystalline $(NH_4)_xWO_3$ nanorods were obtained under mild conditions at a low cost. The formation of the $(NH_4)_xWO_3$ nanorods is also discussed based on time-dependent experiments.

---

2 EXPERIMENTAL PART

In a typical procedure, 3.07 g of $Na_2WO_4 \cdot 2H_2O$, 1.78 g of CH_4N_2S and 1.92 g of $C_6H_8O_7 \cdot H_2O$ were dissolved in 30 mL of deionized water under vigorous stirring for 10 min. The obtained mixed solution was transferred into a 50-mL stainless-steel Teflon-lined autoclave, which was filled with deionized water up to 80 % of the total volume. The hydrothermal treatment was performed by placing the sealed autoclave in an oven and maintaining it at 200 °C for different reaction times. Then the autoclave was taken out and cooled to room temperature in air. The products were filtered and washed with deionized water and ethanol several times in turn, and finally oven dried in air at 60 °C for 12 h.

Powder X-ray diffraction (XRD) patterns of the samples were measured on a D8 advance X-ray diffractometer with high-intensity Cu-K_α (λ = 0.15418 nm) radiation. The surface composition and binding energy of the samples were determined with an Esccalab 250Xi X-ray photoelectron spectrometer (XPS). Scanning-electron-microscope (SEM) images were obtained with a Zeiss Σigma field-emission scanning-electron microscope. Transmission-electron-microscope (TEM) and high-resolution TEM (HRTEM) images were obtained using a FEI Tecnai G2 20 transmission electron microscope at 200 kV.

3 RESULTS AND DISCUSSION

Figure 1a shows the XRD pattern of the as-prepared sample hydrothermally synthesized at 200 °C for 12 h. It was found that all the diffraction peaks could be well indexed to the hexagonal $(NH_4)_xWO_3$ with known lattice constants of a = 0.7388 nm and c = 0.7551 nm (ICDD PDF no. 73-1084), and no characteristic peaks for impurities such as WO_3 or WO_{3-x} were observed. The chemical composition and valence state of the as-prepared $(NH_4)_xWO_3$ sample was examined with XPS. The fully scanned spectra clearly show that N, W, O and C existed in the sample (**Figure 1b**). The presence of carbon in the final product may be related to the residual, chemically or physically adsorbed organics originating from CH_4N_2S or $C_6H_8O_7 \cdot H_2O$. The XPS peak of N1s located at 402.2 eV may be related to the NH^{4+} ions in $(NH_4)_xWO_3$. For tungsten, a complex energy distribution of W4f photoelectrons was obtained, as shown in **Figure 1c**.

After deconvolution, the W4f core-level spectrum could be well fitted to two spin-orbit doublets, corresponding to W atoms in two different oxidation states. The main peaks, W4f$_{5/2}$ at 37.8 eV and W4f$_{7/2}$ at 35.7 eV, could be attributed to the W atoms being in the 6+ oxidation state. The second doublet, with lower binding energies of 34.9 eV and 36.3 eV could be assigned to the emission of the W4f$_{5/2}$ and W4f$_{7/2}$ core levels from the atoms in the oxidation state of 5+. These results for the core level of tungsten ions in tungsten bronze are in good agreement with reported values.[8] The chemical composition determined from the deconvolution of the XPS spectrum is $(NH_4)_{0.25}WO_3$.

Figure 2a presents the SEM images of the as-prepared $(NH_4)_xWO_3$ sample hydrothermally synthesized at 200 °C for 12 h. The sample consisted of numerous nanorods, which were straight and had smooth surfaces, and the average diameter and length of the nanorods were 150 nm and 2 μm, respectively. The obtained $(NH_4)_xWO_3$ nanorods were further characterized with TEM to determine their structural features and understand their crystal-growth behavior.

A low-magnification TEM image of a randomly chosen single $(NH_4)_xWO_3$ nanorod is shown in **Figure 2b**. The selected-area-electron-diffraction (SAED) pattern (inset in **Figure 2b**) of the single nanorod can be indexed to the [010] zone axis of the hexagonal $(NH_4)_xWO_3$, suggesting that the as-prepared $(NH_4)_xWO_3$ nanorods are single crystalline in nature. An HRTEM
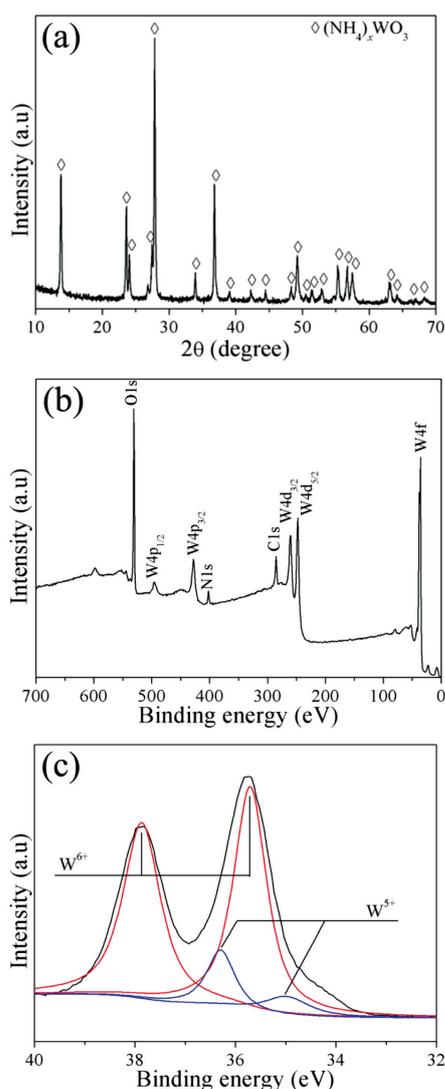
Figure 1: a) XRD pattern, b) full-range XPS spectra and c) W4f core-level XPS spectra of the as-prepared $(NH_4)_xWO_3$ sample
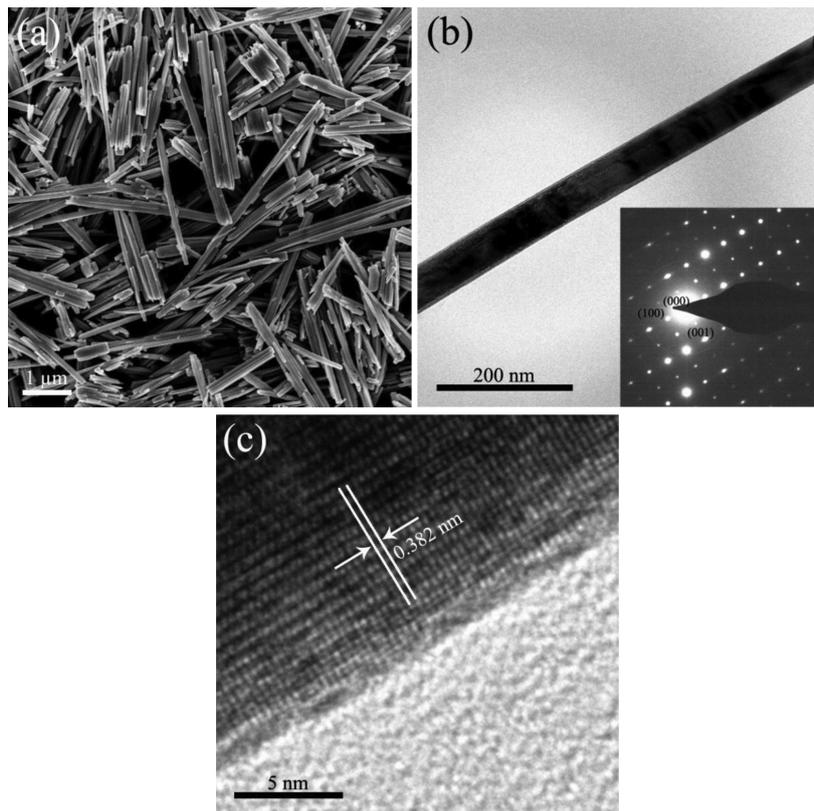
Figure 2: a) SEM image, b) TEM image and c) HRTEM image of the as-prepared $(NH_4)_x WO_3$ sample. The inset shows the corresponding SAED pattern (b)
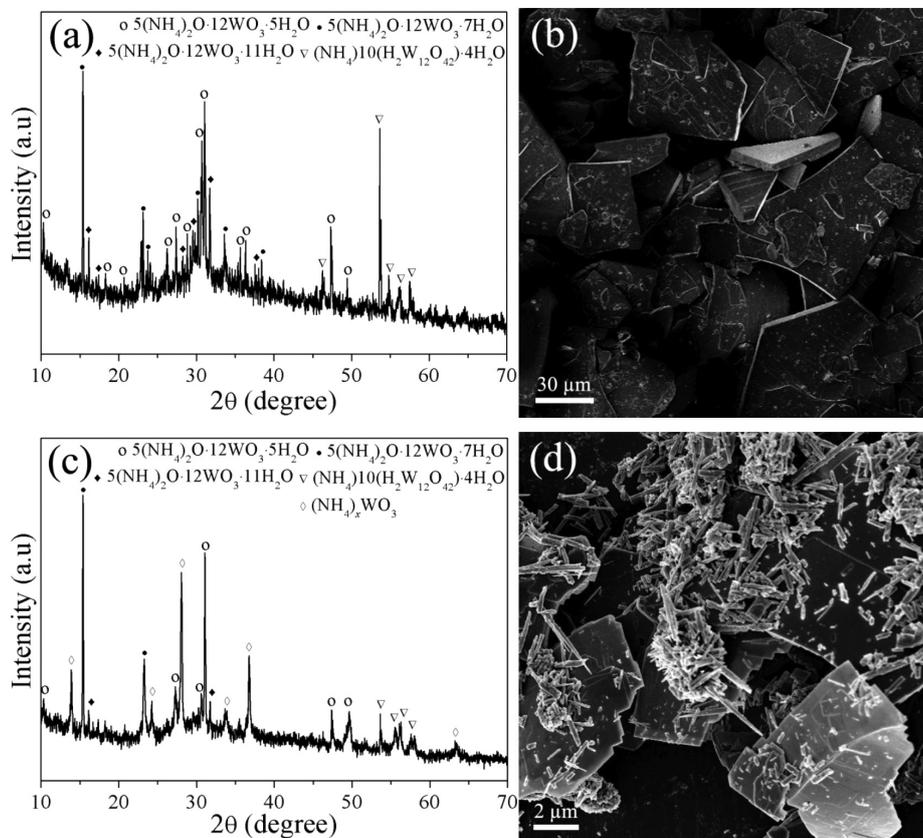
Figure 3: XRD pattern and SEM image of the products after reaction times of: 2 h (a, b) and 6 h (c, d), respectively

image of the $(NH_4)_xWO_3$ nanorod at a greater magnification (**Figure 2c**) shows clear and ordered lattice fringes, confirming that the nanorods are single crystals. In addition, the crystalline-lattice constant in the direction parallel to the nanorod was measured as 0.382 nm, which agrees well with the interplanar spacing of (0 0 2), indicating the preferential growth along the c-axis of the hexagonal bronze structure.

To understand the formation process of the single-crystal $(NH_4)_xWO_3$ nanorods, time-dependent experiments involving changing the hydrothermal reaction time were performed. Initially, the reaction products obtained after 2 h of the hydrothermal treatment were identified as the $5(NH_4)_2O \cdot 12WO_3 \cdot 5H_2O$ (ICDD PDF no. 18-0128), $5(NH_4)_2O \cdot 12WO_3 \cdot 7H_2O$ (ICDD PDF no. 18-0126), $5(NH_4)_2O \cdot 12WO_3 \cdot 11H_2O$ (ICDD PDF no. 18-0127) and $(NH_4)_{10}(H_2W_{12}O_{42}) \cdot 4H_2O$ (ICDD PDF no. 40-1470) phases from their XRD patterns (**Figure 3a**). The chemical formula of these phases can be represented as $5(NH_4)_2O \cdot 12WO_3 \cdot nH_2O$ ($n = 5, 7, 11$). The obtained $5(NH_4)_2O \cdot 12WO_3 \cdot nH_2O$ products display a sheet-like appearance with a lateral size of tens of micrometers (**Figure 3b**). The $5(NH_4)_2O \cdot 12WO_3 \cdot nH_2O$ products were gradually converted into hexagonal $(NH_4)_xWO_3$ due to a certain amount of hexagonal $(NH_4)_xWO_3$ phase, the diffraction peaks of which were detected when the reaction time was extended to 6 h (**Figure 3c**).

The SEM image also demonstrates that the $5(NH_4)_2O \cdot 12WO_3 \cdot nH_2O$ phases dissolved and that species with a rod-like appearance were formed (**Figure 3d**). When the reaction time was extended to 12 h, only $(NH_4)_xWO_3$ nanorods were found in the sample (**Figure 2a**), and no sheet-like $5(NH_4)_2O \cdot 12WO_3 \cdot nH_2O$ phases remained. In addition, as a comparative experiment, when neither CH_4N_2S nor $C_6H_8O_7 \cdot H_2O$ were used in this hydrothermal system, no $(NH_4)_xWO_3$ phases were generated even if the other experimental conditions were maintained.

Based on the above results, the suggested reaction equations in this hydrothermal system are as follows:

$$12WO_4^{2-} + 18H^+ \rightarrow H_2W_{12}O_{40}^{6-} + 8H_2O \qquad (1)$$

$$CH_4N_2S + 2H_2O \rightarrow 2NH_3 + H_2S + CO_2 \qquad (2)$$

$$H_2W_{12}O_{40}^{6-} + 10NH_3 + (n+7)H_2O \rightarrow$$
$$5(NH_4)_2O \cdot 12WO_3 \cdot nH2O + 6OH^- \qquad (3)$$

$$5(NH_4)_2O \cdot 12WO_3 \cdot nH_2O + 2xH_2S \rightarrow 12(NH_4)_xWO_3 +$$
$$+ (10-12x)NH_3 + 2xSO_2 + (n+5-4x)H_2O \qquad (4)$$
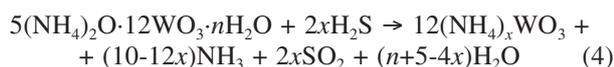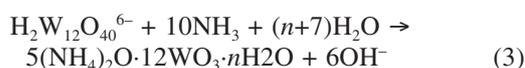
During the initial stage, WO_4^{2-} and H^+ ions were released by $Na_2WO_4 \cdot 2H_2O$ and $C_6H_8O_7 \cdot H_2O$ into the solution, respectively. Then, $H_2W_{12}O_{40}^{6-}$ ions were generated due to the reaction of WO_4^{2-} and H^+,[9,10] as shown with Equation (1). The hydrolysis of CH_4N_2S could produce massive quantities of NH_3 and H_2S under hydrothermal conditions, as expressed with Equation (2). As the reaction time increased, the $H_2W_{12}O_{40}^{6-}$ ions further reacted with NH_3 and H_2O, forming sheet-like
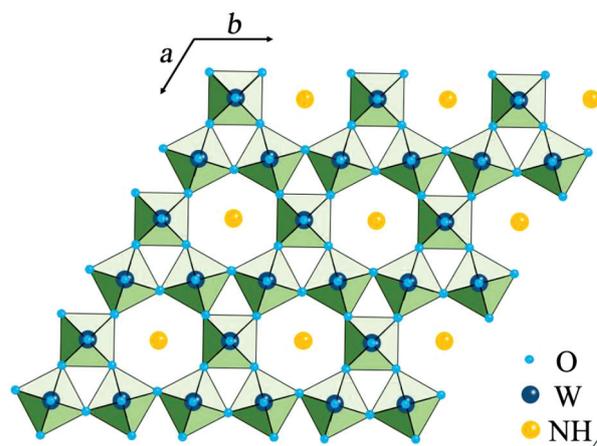
Figure 4: Crystal structure of the as-prepared $(NH_4)_xWO_3$ sample

$5(NH_4)_2O \cdot 12WO_3 \cdot nH_2O$ phases according to Equation (3). As the reaction time progressed further, these sheet-like $5(NH_4)_2O \cdot 12WO_3 \cdot nH_2O$ phases were gradually transformed into $(NH_4)_xWO_3$ nanorods upon an H_2S reduction through a dissolution-recrystallization mechanism.[11,12] The chemical reaction of this process can be expressed with Equation (4). Finally, the pure $(NH_4)_xWO_3$ nanorods were obtained at the expense of a complete consumption of the sheet-like $5(NH_4)_2O \cdot 12WO_3 \cdot nH_2O$ phases (12 h). The oriented growth of the $(NH_4)_xWO_3$ nanorods is associated with their specific crystal structure.

In hexagonal tungsten bronzes (M_xWO_3, $x \leq 0.33$), the structure mainly comprises a rigid tungsten-oxygen framework built of layers containing corner-sharing WO_6 octahedra, which are arranged in six membered rings. The layers are stacked along the c-axis, leading to the formation of one-dimensional open hexagonal channels, which are randomly occupied by cations (**Figure 4**).[13] Therefore, the growth preferentially occurs along the c-axis of the $(NH_4)_xWO_3$ nanorods due to their specific crystal structure.

4 CONCLUSIONS

In summary, single-crystalline $(NH_4)_xWO_3$ nanorods with hexagonal structures were obtained through a novel hydrothermal route at 200 °C, taking 12 h, with $Na_2WO_4 \cdot 2H_2O$, CH_4N_2S and $C_6H_8O_7 \cdot H_2O$ as the starting materials. The as-prepared $(NH_4)_xWO_3$ nanorods had an average diameter of 150 nm and length of 2 μm and they grew along the c-axis. Time-dependent experiments were carried out to further clarify the formation of the $(NH_4)_xWO_3$ nanorods. This study provides a simple, mild and economical route for preparing one-dimensional $(NH_4)_xWO_3$ nanostructures.

Acknowledgment

5 REFERENCES

[1] C. S. Guo, S. Yin, P. L. Zhang, M. Yan, K. Adachi, T. Chonan, T. Sato, Novel synthesis of homogenous $Cs_x WO_3$ nanorods with excellent NIR shielding properties by a water controlled-release solvothermal process, J. Mater. Chem., 20 (**2010**), 8227–8229, doi:10.1039/c0jm01972k

[2] C. S. Guo, S. Yin, M. Yan, T. Sato, Facile synthesis of homogeneous $Cs_x WO_3$ nanorods with excellent low-emissivity and NIR shielding property by a water controlled-release process, J. Mater. Chem., 21 (**2011**), 5099–5105, doi:10.1039/c0jm04379f

[3] C. S. Guo, S. Yin, T. Sato, Synthesis of one-dimensional hexagonal sodium tungsten oxide and its near-infrared shielding property, Nanosci. Nanotechnol. Lett., 3 (**2011**), 413–416, doi:10.1166/nnl.2011.1182

[4] C. S. Guo, S. Yin, L. J. Huang, T. Sato, Synthesis of one-dimensional potassium tungsten bronze with excellent near-infrared absorption property, ACS Appl. Mater. Interfaces, 3 (**2011**), 2794–2799, doi:10.1021/am200631e

[5] C. S. Guo, S. Yin, L. J. Huang, L. Yang, T. Sato, Discovery of an excellent IR absorbent with a broad working waveband: $Cs_x WO_3$ nanorods, Chem. Commun., 47 (**2011**), 8853–8855, doi:10.1039/c1cc12711j

[6] C. S. Guo, S. Yin, Q. Dong, T. Sato, Simple route to (NH₄)$_x$WO₃ nanorods for near infrared absorption, Nanoscale, 4 (**2012**), 3394–3398, doi:10.1039/c2nr30612c

[7] C. S. Guo, S. Yin, T. Sato, Tungsten oxide-based nanomaterials: morphological-control, properties, and novel applications, Rev. Adv. Sci. Eng., 1 (**2012**), 235–263, doi:10.1166/rase.2012.1016

[8] M. Sun, N. Xu, Y. W. Cao, J. N. Yao, E. G. Wang, Nanocrystalline tungsten oxide thin film: preparation, microstructure, and photochromic behavior, J. Mater. Res., 15 (**2000**), 927–933, doi:10.1557/JMR.2000.0132

[9] J. P. Launay, M. Boyer, F. Chauveau, High resolution PMR of several isopolytungstates and related compounds, J. Inorg. Nucl. Chem., 38 (**1976**), 243–247, doi:10.1016/0022-1902(76)80402-2

[10] J. J. Hastings, O. W. Howarth, A ^{183}W, ^{1}H and ^{17}O nuclear magnetic resonance study of aqueous isopolytungstates, J. Chem. Soc. Dalton Trans., 2 (**1992**), 209–215, doi:10.1039/dt9920000209

[11] L. Q. Jiang, Y. Qiu, Z. G. Yi, Potassium niobate nanostructures: controllable morphology, growth mechanism, and photocatalytic activity, J. Mater. Chem. A, 1 (**2013**), 2878–2885, doi:10.1039/C2TA01056A

[12] X. Li, J. L. Zang, Facile hydrothermal synthesis of sodium tantalate (NaTaO₃) nanocubes and high photocatalytic properties, J. Phys. Chem. C, 113 (**2009**), 19411–19418, doi:10.1021/jp907334z

[13] A. Hussain, L. Kihlborg, A. Klug, The transformation between hexagonal potassium tungsten bronze and polytungstate, J. Solid State Chem., 25 (**1978**), 189–195, doi:10.1016/0022-4596(78)90102-0